Experimental investigation on wall pressure distribution in flaps' separating regions

P. F. Zhang, J. J. Wang and Y. C. Li
Institute of Fluid Mechanics,
Beijing University of Aeronautics and Astronautics,
Beijing, Peoples Republic of China

ABSTRACT

The effects on the wall pressure of the plate caused by the introduction of a gap near the ground and the flaps were investigated experimentally. The mean pressure on the plate surface was found to decrease with the size changing of the gap near the ground when the gap size (g) is larger than the flap height (h), but the one in the recirculation region increase with the size of the gap when the gap size is about $0 \le g \le 2h$. Three kinds of flow structure appear with increasing the gap sizes, and the transit point is at g/h = 0·2, 0·8 respectively. For the zigzag flap (d/h = 0·19, d is the height of the zigzag), the variation of wall pressure with g/h is similar to the flat flap in general. The zigzag affects the mean wall pressure in the region of $0 \le x/h \le 20$ (the recirculation zone) and can decrease the fluctuating pressure in the region of $x/h > 20$ downstream.

NOMENCLATURE

c	chord length
C_p	mean wall pressure coefficient (= $(p-p_\infty)/0{\cdot}5\rho U_\infty$)
C_{pmax}	the maximum pressure coefficient upstream of the flap
C_{pmin}	the minimum pressure coefficient downstream of the flap
d	zigzag height
g	gap size between the plate surface and the bottom of flap
h	flap height
p	mean static pressure
p'	fluctuating pressure
p_0	free stream pressure
P'	fluctuating pressure coefficient (= $p'/0{\cdot}5\rho U_\infty$)
$\mathrm{Re_h}$	Reynolds number based on the height of the flap (= $U_\infty h/\nu$)
U_∞	free stream velocity
x	axial distance downstream of the flap
θ	inclination of the flap
α	attack angle of the aerofoil
δ	boundary-layer thickness
η	fence porosity
ρ	density of the fluid
ν	kinematic viscosity of the fluid

1.0 INTRODUCTION

Separating and reattaching flows are encountered in diverse fields. For example, agricultural engineers dealing with shelterbelts, hydraulic engineers involved in the design of spur, and aerodynamicists dealing with tall buildings exposed to atmospheric boundary-layer flow. The spread of polluted air in the vicinity of buildings and disposal of the polluted water into rivers are problems of similar nature dealing by environmentalists. Porous wind fences have been used in many practical applications instead of solid fence. Experimental and CFD studies found that fences with porosity η = 20% can decrease the turbulence intensity downstream of the fences[1–5]. But the problem is the porous fences with circular holes are not easy to manufacture in applications.

Paper No. 2833. Manuscript received 13 March 2003, accepted 29 July 2003.

https://doi.org/10.1017/S0001924000005054 Published online by Cambridge University Press

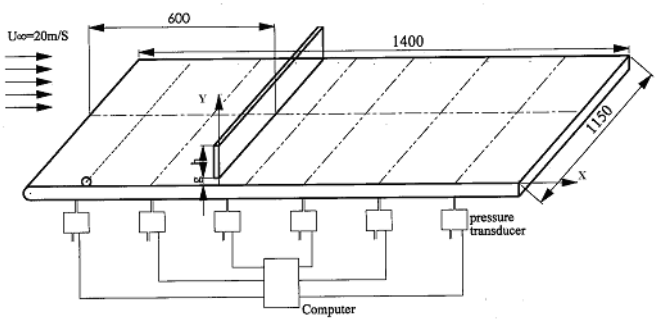


Figure 1. Experimental setup.

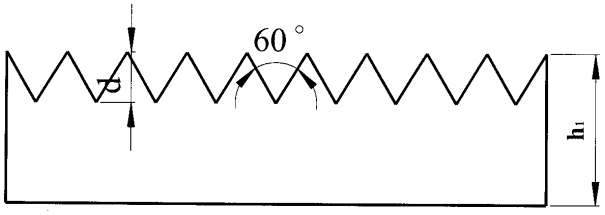


Figure 2. The zigzag flap.

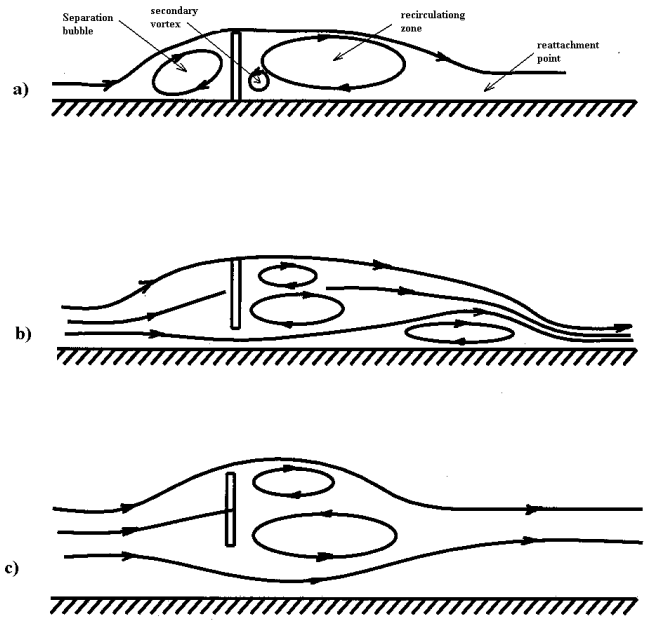


Figure 3. Three typical flow structures.

Table 1
The size of the sawtooth flap

d/h	0·19	0·33	0·46	0·57	0·67
d(mm)	2·0	4·0	6·0	8·0	10·0
h(mm)	11	12	13	14	15

Spoiler is usually deployed rapidly during landing of aircrafts to reduce the lift and to increase the drag. However, in addition to having a considerable time lag, the solid-type spoiler also induces an initial increase in lift and decrease in pitch moment before reaching its long-term values. These adverse phenomena are attributed to the vertical of a starting vortex shed from the spoiler tip. Yeung *et al*[6] took plenty of experiments at $Re_h = 3{\cdot}5 \times 10^5$ and the relative gap sizes g/c = 0%, 2%, 4·9%, 7·2%. They found base venting can change the flow structures downstream of the spoiler from a recirculating zone to a wake because of the shear layer from lower tip. It can not only decrease the static lift and pitch moment at $\theta = 90°$ with the attack angle of $\alpha = 0°$, 5°, 10°, 20°, but also reduce the transient adverse effects significantly. For the relative gap size g/c = 7·2, the adverse lift coefficient and pitch moment coefficient decrease below 0·05. Then Yeung *et al*[7] chose forward-facing flap to reduce the transient adverse effects of the spoiler. The experimental Reynolds number is $Re_h = 6{\cdot}45 \times 10^3$, and the relative boundary-layer thickness δ/h is 0·4. The flow structure of the forward-facing flap (with or without base-venting) is similar to the spoiler mounted on aerofoils. They can both increase the drag and decrease the lift, furthermore, the forward-facing flap can reduce the transient adverse effects significantly. So Yeung *et al*[6,7] advised to use forward-facing flap in stead of the spoiler for the purpose reducing the transient adverse effects.

The base venting flap concentrates the porosity to the gap, it may have the same function as the porous fence. The zigzag can tear the vortex sheet separated from the upper tip of the flap, so many eddies appear in the downstream. These eddies can consume more power of the flow than that of flat flap, so the fluctuation of the pressure can also decrease. This paper studies the effects of different gap sizes and heights in the zigzag on the mean wall pressure behind the flaps. The fluctuating pressure behind the zigzag flap is also investigated. The main contents are as follows: The base-venting effects on the wall pressure induced by the flat flap. The base-venting effects on the wall pressure induced by the zigzag flap of d/h = 0·19. The effects of zigzag height on the wall pressure induced by zigzag flaps.

2.0 EXPERIMENTAL SETUP AND TECHNOLOGY

The pressure measurements is carried out in D1 wind tunnel (open-circuit wind tunnel) of Beijing University of Aeronautics and Astronautics. The entrance and exit of the test section are all elliptical, with the sizes 1·02m × 0·76m and 1·07m × 0·81m, respectively. There is an organic glass plate below the model, with size of 1,400mm × 1,150mm × 15mm. The flaps is mounted 600mm from the tip of the base plate, and a two-dimensional trip wire is placed at the location of 6mm from the tip of the base plate to get boundary-layer transition early. At the position of flap, the turbulence boundary-layer thickness is about d/h = 1·4. In this experiment, six aluminium alloy flap models were chosen, one size of the flat flap is 600mm × 10mm × 1·5mm and the other five zigzag flaps' relative height are d/h = 0·19, 0·33, 0·56, 0·57, 0·67. The effective area of the zigzag flap is equal to that of the flat flap. The velocity of the freestream is $20ms^{-1}$, and Reynolds number Re_h based on the height of the model is $1{\cdot}26 \times 10^4$. The gap sizes g/h are 0, 0·2, 0·4, 0·6, 0·8, 1·0, 1·5, 2·0, 3·0, 4·0, 5·0, respectively. Thirty holes of diameter 1·2 mm are drilled at various streamwise positions symmetrically of the base plate and served as pressure ports, x = –110, –90, –70, –50, –40, –30, –20, –10, 10, 20, 30, 40, 60, 80, 100, 120, 140, 160, 180, 200, 220, 240, 260, 280, 300, 320, 340, 360, 380, 400mm. The experimental setup is shown in Fig. 1, the size of the zigzag flap is listed in Table 1 below.

Thirty pressure taps are connected with the pressure scan model of Hyscan2000 system by plastic tubings with inner diameter of 0·8 (mm), the length of the tubing is 500mm. The error of the pressure value is about 0·0002PSI.

https://doi.org/10.1017/S0001924000005054 Published online by Cambridge University Press

3.0 EXPERIMENTAL RESULT AND DISCUSSION

3.1 The effect of different gap sizes on the mean wall pressure induced by the flat flap

The flow around a flat flap ($g/h = 0$) mounted on the surface of plate is characterized by an upstream region of gradual rise in pressure, where $C_p > 0$, and a downstream region of rising pressure, but with $C_p < 0$. The flow structure is shown in Fig. 3(a). An upstream separation bubble can be easily found near the front base of the flat flap as a result of flow deceleration leading to boundary-layer separation. A recirculation zone, which is bound by the shear layer emanating from the tip of flat flap and terminated at a reattachment point on the flat surface, is the flow structure behind the flat flap. The wall pressure accordingly has a large suction ($0 \le x/h \le 20$) downstream of the flat flap as seen in Fig. 4. The recirculation zone is easily detected by pressure measurements, the bubble which is generally smaller in size. In the downstream region near the flat flap, the wall pressure distribution persists almost the same trend, and the minimum wall pressure occurs in this recirculation zone.

When there is a base venting between the flat flap and the plate, the fluid upstream enters the recirculation region downstream of the flat flap from the gap like a jet. When the gap is small ($g/h < 0{\cdot}2$), the jet intensity is weaker than the reverse flow in the recirculation zone. It can't blow the main vortex away, so the recirculation zone still exists behind the flat flap. But the intensity of the main vortex decreases and its location is a little farther from the flat flap. In this case, there are two vortices shed from the tips of the flat flap as seen in Fig. 3(b). The wall pressure (seen in Fig. 4) reflects these flow characteristics. A peak of wall pressure appears much closer to the flat flap ($x/h = 2{\cdot}0$), meanwhile the wall pressure upstream and downstream of the flat flap decrease.

When the size of gap is increased but no more than $0{\cdot}8h$ ($0{\cdot}2 \le g/h \le 0{\cdot}8$), the jet becomes stronger and stronger. At this time the jet intensity is stronger than the reverse flow in the recirculation zone, so the recirculation zone doesn't exist any longer. We can find two vortices shed only from the tips of the flat flap(shown in Fig. 3(c)). The wall pressure has a smaller suction ($0 \le x/h \le 6{\cdot}0$) and the minimum wall pressure appears at $x/h = 2{\cdot}0$. When the flat flap is kept away from the plate surface, more fluid upstream enters to downstream and the vortex shedding from the lower tip of the flat flap becomes stronger. So the wall pressure upstream decreases but the absolute value of wall pressure downstream increases, especially where close to the flat flap (seen in Fig. 4).

For the gap sizes larger than $0{\cdot}8h$ ($g/h > 0{\cdot}8$), the vortex intensity, shedding from the lower tip of the flat flap, does not increase any more. But it becomes farther from the plate surface, so the minimum of the wall pressure in suction becomes smaller as shown in Fig. 4, the same time wall pressure upstream of the flat flap is also smaller. When the gap size increases to $6{\cdot}0h$, the flat flap almost has no influence on the wall pressure distribution.

The minimum pressure coefficient C_{pmin} varies with the gap size g as shown in Fig. 5. The variation is mainly in the region of $0 \le g/h \le 2{\cdot}0$, and it also presents the three kinds of typical flow structures of the flat flap. We can see that the C_{pmin} curves have a discrete point at $g/h = 0{\cdot}2$ and the peak value of C_{pmin} appearing at $g/h = 0{\cdot}8$. When the gap size is $g/h = 2{\cdot}0$, the flow structure doesn't change, but the vortex shedding from the lower tip of the flat flap has a little effect on the wall pressure, C_{pmin} recovers to the zero with the gap size g increased slowly.

Figure 6 shows the maximum pressure coefficient $C_{p\max}$ varying with the gap size g .When the gap size is $0 \le g/h \le 1{\cdot}0$, the curves of $C_{p\max}$ have little variation. As the gap size g increases to $1{\cdot}0 \le g/h \le 2{\cdot}0$, $C_{p\max}$ decreases with g increasing distinctly. When the gap size is $2{\cdot}0 \le g/h \le 5{\cdot}0$, the variation of $C_{p\max}$ with the increase of g/h becomes little. The wall pressure in Fig. 4 also has the same trend with $C_{p\max}$, so does the variation of $C_{p\max}$.

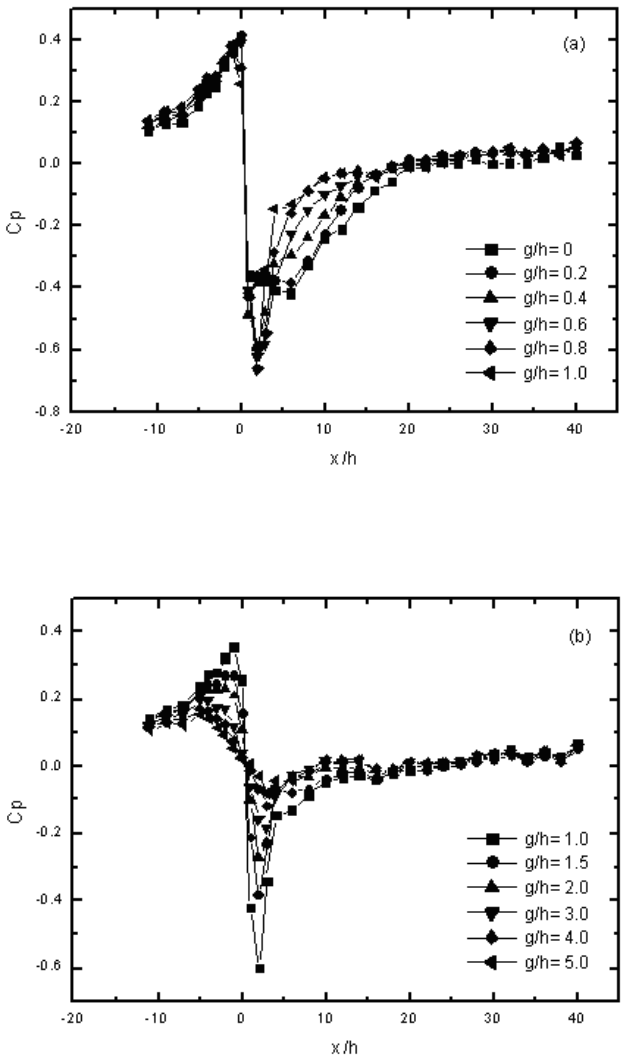


Figure 4. Wall pressure of the flat flap (g/h = 0~6·0).

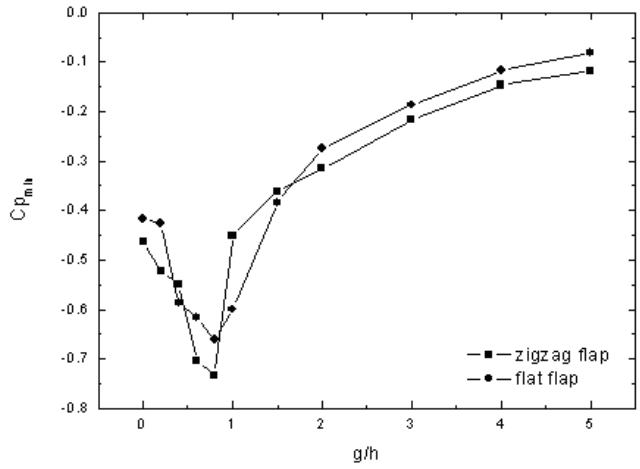


Figure 5. The influence of the gap size g on the minimum pressure coefficient C_{pmin}.

https://doi.org/10.1017/S0001924000005054 Published online by Cambridge University Press

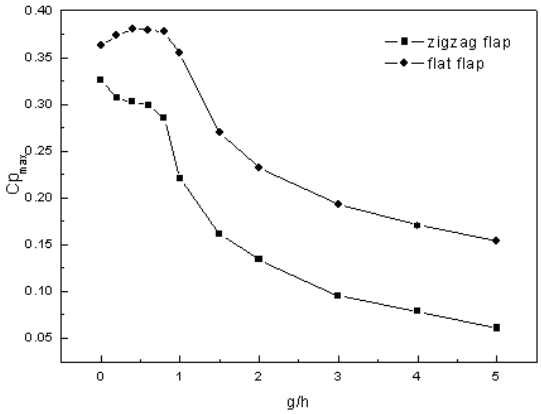


Figure 6. The influence of the gap size g on the maximum pressure coefficient C_{pmax}.

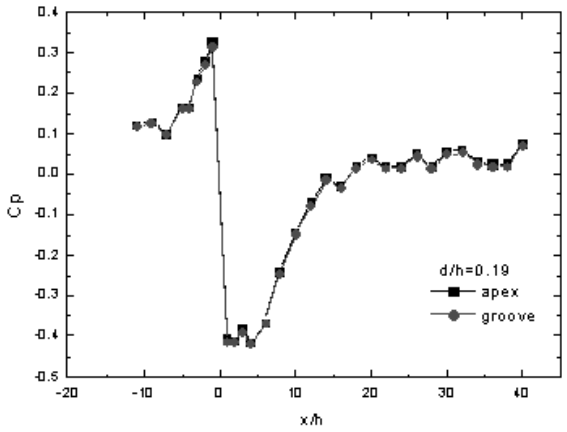


Figure 7. Wall pressure at various transverse locations of d/h = 0·19 zigzag flap.

3.2 The effect of different gap sizes on the mean wall pressure induced by the zigzag flap at d/h = 0·19

3D characteristics appear in the case of flow around the zigzag flap, the wall pressure on the plate surface may have some difference in transverse locations. The distributions of wall pressure along two transverse locations have been measured in this experiment at first, one is along the apex of the zigzag flap and the other is along the groove. Wall pressure of the two cases is presented in Fig. 7, and little difference can be found between them. So wall pressure of the flow around the zigzag flap also has 2D characteristics and the effects of the transverse location of the zigzag flap on the wall pressure can be ignored in the experiment.

When the model has the zigzag at the upper tip, the shear layer around the zigzag flap is not in the same line, and the flow structure is more turbulent. In this case there is a gap between the lower tip of the zigzag flap and the plate surface, the vortex sheet shedding from the upper tip may be teared by the zigzag, but the lower one is still a 2D vortex sheet like that of the flat flap. So the influence on the wall pressure of the zigzag flap is similar to that of the flat flap.

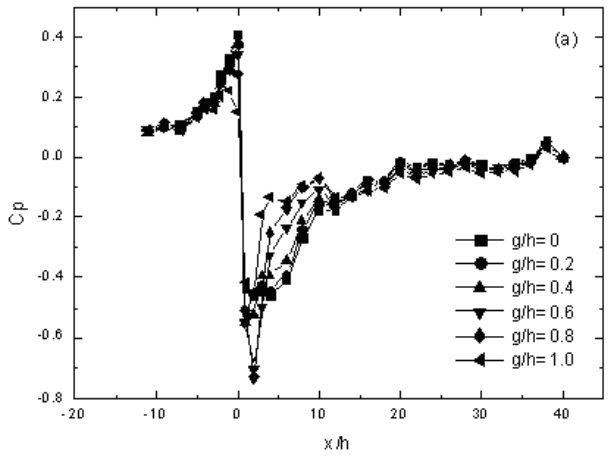
Figure 8 presents the wall pressure of the zigzag flap (d/h = 0·19) with various gap sizes. In general, the variation of wall pressure with the change of g/h is the same as that of the flat flap, but there exists some difference in details. The zigzag flap tears the vortex sheet sheded from the upper tip, the flow downstream of the zigzag flap fluctuates violently, and the dissipation is also much stronger. Thus the vortex behind the zigzag flap becomes weaker than the flat flap case. Wall pressure of the flat flap has a large suction ($0 \le x/h \le 20$) at $g/h \le 0{\cdot}2$, but for the zigzag flap the suction becomes smaller.

The base-venting effects on the C_{pmin} downstream of the zigzag flap is similar to that of the flat flap, but the trend is slow at $g/h \le 1{\cdot}2$ as seen in Fig. 5. The C_{pmax} upstream of the zigzag flap decreases with increasing the gap size g monotonously, and the strongest variation occurs in the region of $0{\cdot}8 \le g/h \le 1{\cdot}5$. The gap size g has little effects when it is too big or too small (See Fig. 5 and Fig. 6).

3.3 The effects of different zigzag heights on the wall pressure distribution

When the model has the zigzag at upper tip, the curve of wall pressure distribution upstream has little variation, and it also has little effects on the wall pressure in the region $x/h \le 20$ downstream of the zigzag flap(seen in Fig. 9). The zigzag effects are mainly in the region $0 \le x/h \le 20$ (the recirculation region), especially in the region where is close to the zigzag flap downstream of the zigzag flap.

Figure 10 presents the fluctuating pressure of the flaps. The fluctuating pressure of the flat flap at the zone $x/h < -4$ mainly depends on the free stream turbulence intensity (P' = 1%), and it increases rapidly at the location of $x/h = -4$ where is the separation point of the boundary layer. There are four peaks of pressure downstream of the plate flap at x/h = 1, 6, 22, 38. The pressure at x/h = 22 is maximum since the boundary layer reattaches to the base plate at this point. The main vortex core and secondary vortex core is at x/h = 1, 6 respectively, and the point of x/h = 38 is the location of secondary reattachment. When the vortex in the shear layer reattaches to the flat plate, a boundary layer develops perpendicular to the axis of the vortex at the wall. The descent of the vortices creates a strong



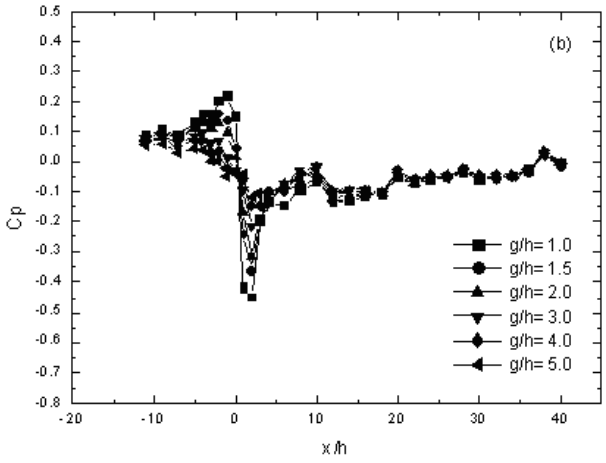


Figure 8. Wall pressure of the zigzag flap at d/h = 0·19 (g/h = 0~6·0).

https://doi.org/10.1017/S0001924000005054 Published online by Cambridge University Press

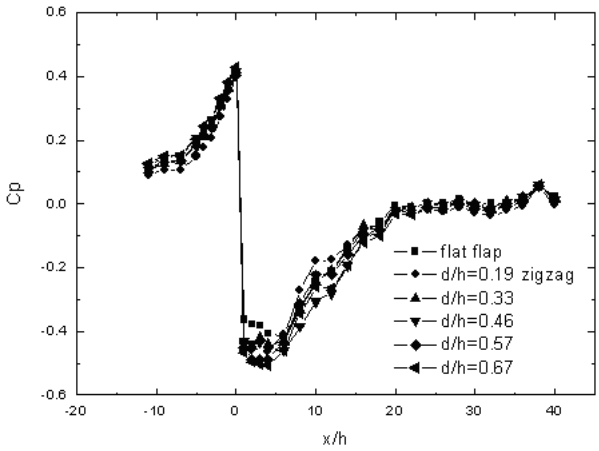


Figure 9. The influence of the height of the zigzag on the mean wall pressure.

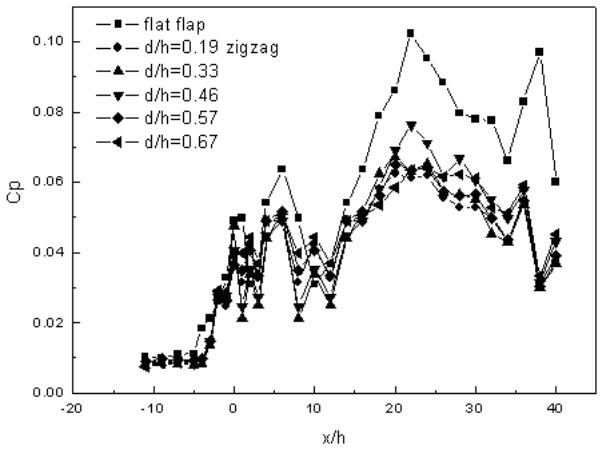


Figure 10. The influence of the height of the zigzag on the fluctuating pressure.

transverse pressure gradient within this boundary layer making it separate. This separation gives rise to a vortex known as the secondary vortex. Its size increases quickly, thus pushing up the primary vortex[8]. The rebounded vortex reattaches to the flat plate downstream, that forms the secondary reattachment.

The zigzag flaps' effective area is equal to that of the plate flap, so the fluctuating wall pressure upstream is the same with that of the flat flap. But the zigzag can decrease the fluctuating pressure in the region $x/h > 20$ downstream of the flap.

4.0 CONCLUSION

The experiment results indicate that the base-venting affects the wall pressure upstream of the flat flap when the gap size is larger than the flap height ($g/h > 1{\cdot}0$) and the wall pressure in the recirculation region downstream mainly at $0 \leq g/h \leq 2{\cdot}0$. There are three kinds of typical flow structures appeared with the increase of gap size exactly at $g/h = 0{\cdot}2$, $0{\cdot}8$. The base-venting effects on the wall pressure induced by the zigzag flap at $d/h = 0{\cdot}19$ is similar to that of the flat flap, but the pressure coefficient C_P downstream varies with the gap size g more than that of the flat flap. The height of zigzag mainly affects the wall pressure induced by the zigzag flap in the recirculation region and can decrease the pressure fluctuation in the region of $x/h > 20$ downstream.

REFERENCES

1. BRADLEY, E.F. and MULHEARN, P.J. Development of velocity and shear stress distributions in the wake of a porous shelter fence. *J Wind Eng and Industrial Aero*, 1983, **15**, (1), pp 145-156.
2. RANGARAJU, K.G., GARDE, R.J., SINGH, S.K. and SINGH, N. Experimental study on characteristics of flow past porous fences. *J Wind Eng and Industrial Aero*, 1988, **29**, (1), pp 155-163.
3. YARAGAL, S.C., GOVINDA, H.S. and MURTHY, K.K. An experimental investigation of flow fields downstream of solid and porous fences. *J Wind Eng and Industrial Aero*, 1997, **66**, (1), pp 127-140.
4. LEE, S.J. and KIM, H.B. Laboratory measurements of velocity and turbulence field behind porous fences. *J Wind Eng and Industrial Aero*, 1999, **80**, (2), pp 311-326.
5. FANG, F.M. and WANG, D.Y. On the flow around a vertical porous fence. *J Wind Eng and Industrial Aero*, 1997, **66/68**, (4), pp 415-424.
6. YEUNG, W.W.H., XU, C. and GU, W.D. Reduction of transient adverse effect of spoilers. *J Aircr*, 1997, **34**, (4), pp 479-484.
7. YEUNG, W.W.H. and XU, C. Separated flows around spoilers and forward-facing flaps. *J Aircr*, 1998, **35**, (1), pp 53-59.
8. HARVEY, J.K. and PERRY, F.J. Flowfield produced by trailing vortices in the vicinity of the ground, *AIAA J*, 1971, **9**, (8), pp 1659-1660.

https://doi.org/10.1017/S0001924000005054 Published online by Cambridge University Press